Impact of Aging on PIM and DC Resistance of Fabric-over-Foam Metallic Contacts

Kalkidan W. Anjajo^{#1}, Seunghun Ryu^{#2}, Shengxuan Xia^{#3}, Gracie Boyer^{*4}, Yuchu He^{*5}, Haicheng Zhou^{*6}, Hanfeng Wang^{*7}, Jonghyun Park^{*8}, and Chulsoon Hwang^{#9}

*EMC Laboratory, Missouri University of Science and Technology, Rolla, MO, USA
*Google LLC, Mountain View, CA, USA

*Mechanical and Aerospace Engineering, Missouri University of Science and Technology, Rolla, MO, USA

lkah5w@mst.edu, hwangc@mst.edu

Abstract— In this paper the impact of aging on the level of passive intermodulation (PIM) and DC resistance of fabric-over-foam metallic contacts is presented. These contacts are widely used to maintain metallic connections between modules and chassis in electronic devices. The PIM caused by the loose metallic contact of these materials mainly affects a receiver's RF sensitivity in mobile devices. This aging test under elevated temperature and relative humidity conditions offers an experiment-based approach with respect to various metallic contact cases. Energy dispersive spectroscopy and scanning electron microscopy are used to characterize the change in material composition and the contact surface throughout the aging. The experimental environmental effects showed the aging on the generated PIM level to have little to no impact from weakened adhesive contact and an increase in lowest PIM floor. Also, an increase in DC resistance level of these metallic contact materials was observed due to an oxide growth on the fabric-over-foam surface.

Keywords—aging, fabric-over-foam (FOF), passive intermodulation (PIM), DC resistance (DCR)

I. INTRODUCTION

Frequency division duplex systems use two different radio frequencies (RFs) to transmit and receive at the same time and share the same antenna. Because of passive intermodulation (PIM), the intermodulation products of the transmitted signals may enter the receiver's spectrum and reduce its sensitivity [1]-[3]. PIM distortion is one of the critical issues in smartphones and many wireless devices [4]. Loose metallic contacts of spring clips and fabric-over-foams (FOFs) are primary contributors towards PIM generation when utilized for electrical connections in modern consumer electronics designs.

Fabric-over-foams are metallic structures which are similar to electromagnetic interference (EMI) gaskets. The conductive fabric part is produced by coating a nonconductive fabric with conductive material, using different coating techniques [6]. The elemental composition of the conductive surface can be obtained using energy dispersive spectroscopy (EDS) analysis. From EDS analysis, it has been found that nickel is the base metal of the FOF type used throughout this paper. According to [7], nickel plating is employed to increase physical qualities, such as wear resistance, heat resistance, or corrosion resistance.

Nickel coatings play a crucial function in a variety of applications by enhancing corrosion resistance.

Corrosion and oxidation on the surface of metals are among the major barriers to maintain good metallic connections. The growth of the oxide layer varies depending on the specific metal type and the extent of environmental exposure. These unintentional barriers not only affect signal flow at RFs, but also potentially affect the current flow at a DC. In [5], the effects of aging on the electrical resistance of gold-nickelcopper connectors are studied: three mechanisms of environmental aging have been implemented to age the samples, namely mixed flowing gas (MFG), elevated temperature, and relative humidity (TRH) and thermal cycling (TC). Results from this study show a dramatic increase in contact electrical resistance throughout the environmental aging. In [8], shielding effectiveness (SE) performance together with aging data of an elevated TRH has been found vital for EMI gasket performance evaluation. The study was focused only on SE and no data has been shown for SE variation across various loads.

In mobile phone applications, FOF metallic contacts are assembled within the chassis and the exposure of these contact materials to the environmental air is yet unavoidable after the full phone assembly. However, there has not been any work published regarding the impact of aging on PIM and DC resistance of FOF metallic contacts in electronic device applications.

In this paper, an elevated TRH aging mechanism is considered to characterize the exposure of the FOF metallic contacts to the environment. Seventy-two hours of aging test is conducted using a temperature-humidity climate chamber. The impact of environmental aging on PIM, DC resistance and hardness of the metallic contacts are studied.

II. MEASUREMENT SYSTEM

A. Test Setup

A measurement setup from [9] is adapted to conduct the PIM measurement. As shown in Fig. 1(a), the FOF metallic contact was used for providing an electrical connection between two pieces of etched aluminum plates cut out from an actual phone chassis (landing pads). These landing pads were each soldered on printed circuit boards with a 50-ohm microstrip

This work was supported in part by Google LLC and the National Science Foundation (NSF) under Grant No. IIP-1916535.

structure as shown in Fig. 1(b). The bottom board was connected to the antenna port of the duplexer and the top one was terminated by a 50-ohm low PIM load. The FOF had an adhesive part on the bottom surface allowing it to stick to the metal chassis of the bottom board, while the upper connection was maintained by sweeping the contact force from loose to good metallic contact.

Two tone sinusoidal signals were generated using signal generators, one at 824 MHz and other at 849 MHz, each amplified and then combined as shown in Fig. 1(a). The combined signal was fed into the Tx port of the duplexer. The output from the antenna port was connected to the DUT(FOF) and the Rx port was connected to a spectrum analyzer (SA) to read the amplitude of the intermodulation product. Only the third-order intermodulation product (IP3) at $2f_2 - f_1$ was measured.

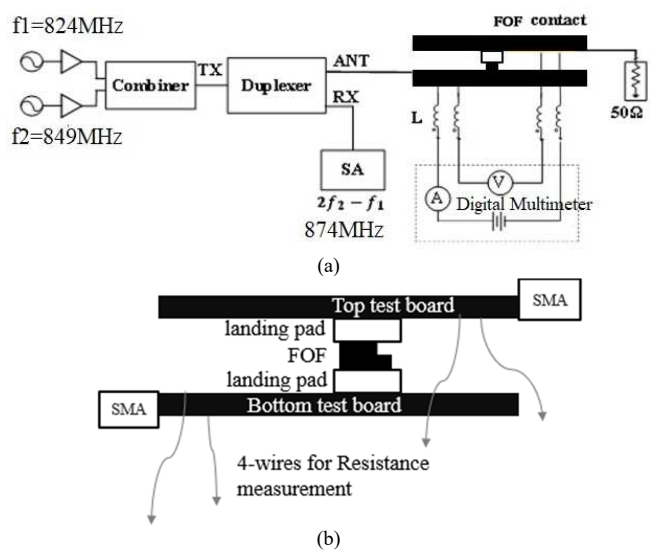


Fig. 1. Test set-up: (a) PIM measurement (b) DC resistance (DCR) measurement.

In addition to characterizing the PIM change at RF, a 4-wire measurement setup (Kelvin connection) adapted from [10] was used to understand the variation of the contact resistance at DC. The four wires were connected to the microstrips right next to the DUT and the resistance reading was obtained by a digital multimeter as shown in Fig. 1(b) at various level of contact forces.

The FOF material used for metallic connection in today's electronic devices are made up mainly of three structures as shown in Fig. 2. The conductive fabric material is composed of various elements such as nickel. EDS analysis was used to understand the elemental composition of the tested conductive fabric surface and the results are shown in Table I.

To understand the actual aging of these metallic contacts due to environmental exposure, aging the materials by an elevated TRH method was applied for this study. A temperature-humidity climate chamber of Model No.: RG-HL-50 from Dongguan Kunlun Industrial Technology Co. was used for this experiment. This climate chamber has a temperature range that

goes up to 85 °C and a humidity range of 20-98% RH (relative humidity) which allows aging tests to be conducted by adjusting the conditions depending on the user requirement.

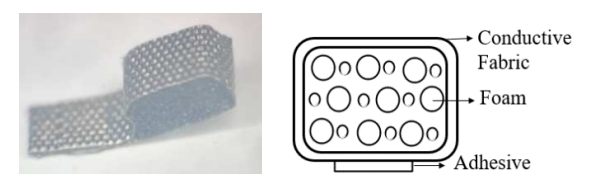


Fig. 2. FOF structure used in the aging tests.

TABLE I. ELEMENTAL COMPOSITION OF THE CONDUCTIVE FABRIC SURFACE OBTAINED FROM EDS ANALYSIS

Element	Weight %
С	7.51
N	1.25
0	4.26
Cl	1.48
Со	1.71
Ni	81.86
Pd	1.93
100	

B. Test Procedure

a) PIM and contact DC resistance measurement: Two rounds of PIM and DC resistance data were taken before and after aging the samples to have a clear comparison for understanding the aging effect. A set of fresh nickel-based FOF samples which had been fabricated recently were prepared to conduct this study. The PIM (IP3) levels sweeping the contact force were measured at 20 dBm input power to the metallic junction and the contact DC resistance was recorded from the digital multimeter at each corresponding contact force. The contact force was swept from zero (no contact) to 0.65 N (well-maintained contact) using a step motor. The maximum force was set to be not greater than 0.65 N to avoid plastic deformation. Fig. 3. Shows the PIM-force and DCR-force plots before the samples go underwent aging.

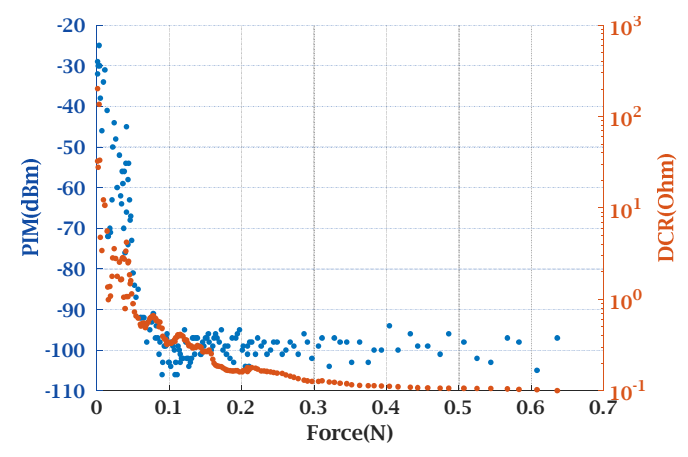


Fig.3. Fresh (unaged) FOF measurement data: PIM-force and DCR-force.

In addition to the PIM and contact DC resistance, force-step curve data was recorded to understand the change in flexibility of the FOF throughout aging. A force-step curve shows the amount of force needed to press the samples to a certain distance. This distance is measured from the reference point (bare contact of the landing pad and the FOF) to the distance at higher contact force. As these samples are made up of a foam, a higher relative humidity was expected to affect the hardness of the material.

b) Aging of the FOF: After the PIM and DCR data were taken for the prepared set of fresh samples, the samples were placed in the climate chamber for accelerated aging. This study focused only on the aging of the FOF material itself and the aging effect while the material was in contact with the metal chasis was not considered. The samples were placed on an acryl plate to avoid any changes resulting from chemical reactions to a metallic surface. The test condition were set to 65 °C and 90% RH. The samples were placed once the chamber was warmed up and equilibrated to the above test condition.

After seventy-two hours of aging, the test samples were taken out of the climate chamber and air blown for drying before conducting the PIM and DC resistance measurement again. No heat was applied while drying the sample to avoid an additional factor towards the recorded measurement data. The test procedure for conducting the measurement is shown in Fig. 4. with a flow chart.

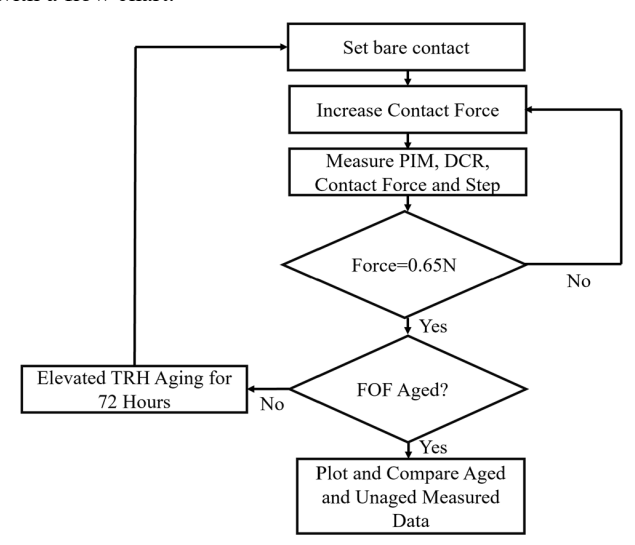


Fig. 4. Flow chart of the aging test.

III. MEASUREMENT DATA AND ANALYSIS

Two data collection methods were implemented. The first one was to track the aging effect every twenty-four hours for three days, while the second one was to track the changes only once fully aged for seventy-two hours.

Although tracking the variation in PIM and DC resistance every 24 hours was expected to help to understand the whole aging process impact, it was found that the frequent assembly and removal of the FOF from the metal chassis reduced the contact strength of the adhesive. The spikes in PIM level were observed at a higher contact force as shown in Fig. 5(a). These

higher-level IP3 values were caused due to the weak adhesive contact resulting in the tail part of the FOF forming a curvature and creating unintentional contact with the upper metal landing pad. An insulation tape (Kapton tape) was used to avoid this unintentional contact and the samples were measured again. As shown in Fig. 5(b), the results show no higher PIM spikes at a good contact region with the insulation tape, as there was no more tail-upper landing pad unintentional contact. The tail-upper landing pad contact is well demonstrated below in Fig. 6. The left-hand side(a) shows fresh FOF with strong adhesive and the right-hand side(b) shows the unintentional contact after the adhesive got weaker.

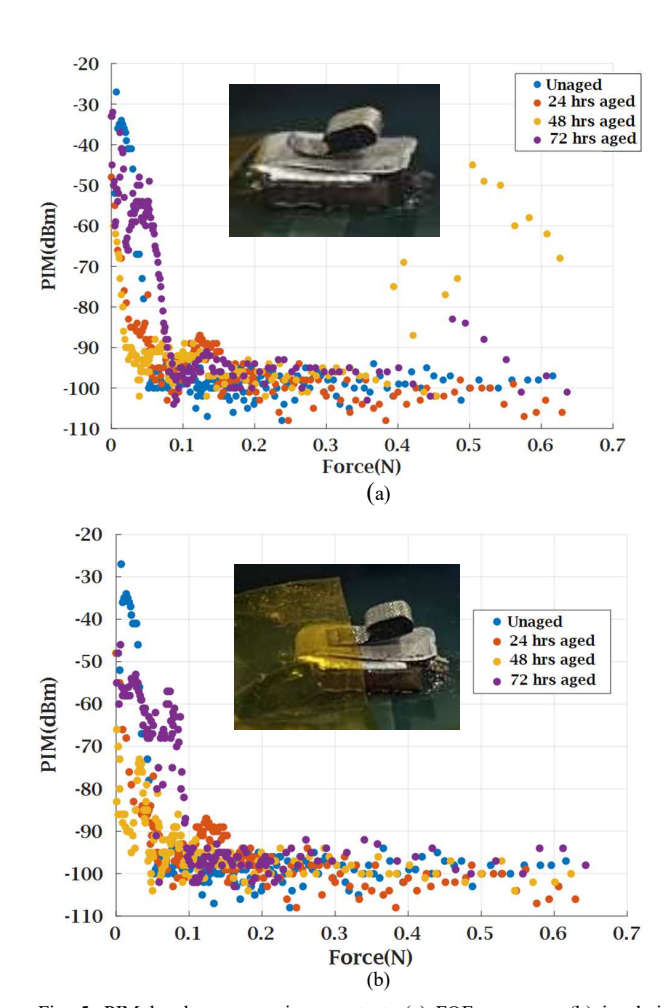


Fig. 5. PIM level across various contacts (a) FOF curvature (b) insulation (Kapton tape) used to avoid the curvature touching the upper landing pad.

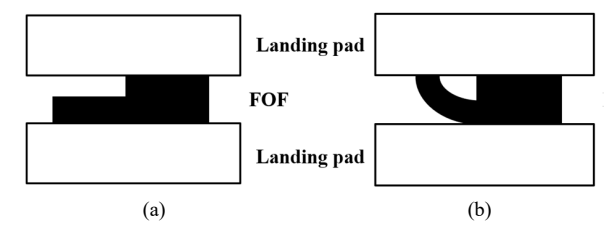


Fig. 6. FOF-landing pad contact: (a) fresh FOF (b) tail-landing pad contact after frequent removal and assembly

In the second scenario, the FOF samples were continuously kept in the climate chamber for seventy-two hours. The PIM and DC resistance data measured from 14 samples are plotted in Fig. 7. The impact of the aging on the PIM level was found to have little to no effect on most cases. For the rest of the cases, an increase in lowest PIM floor was observed and the data is shown in Fig. 7(a). Also, the tail-upper landing pad contact effect was observed again indicating the adhesive on the bottom surface of the FOF became less sticky resulting in the curvature of the tail from weaker contact. Fig. 7(b) shows the increase in DC resistance of the samples throughout aging for all the cases.

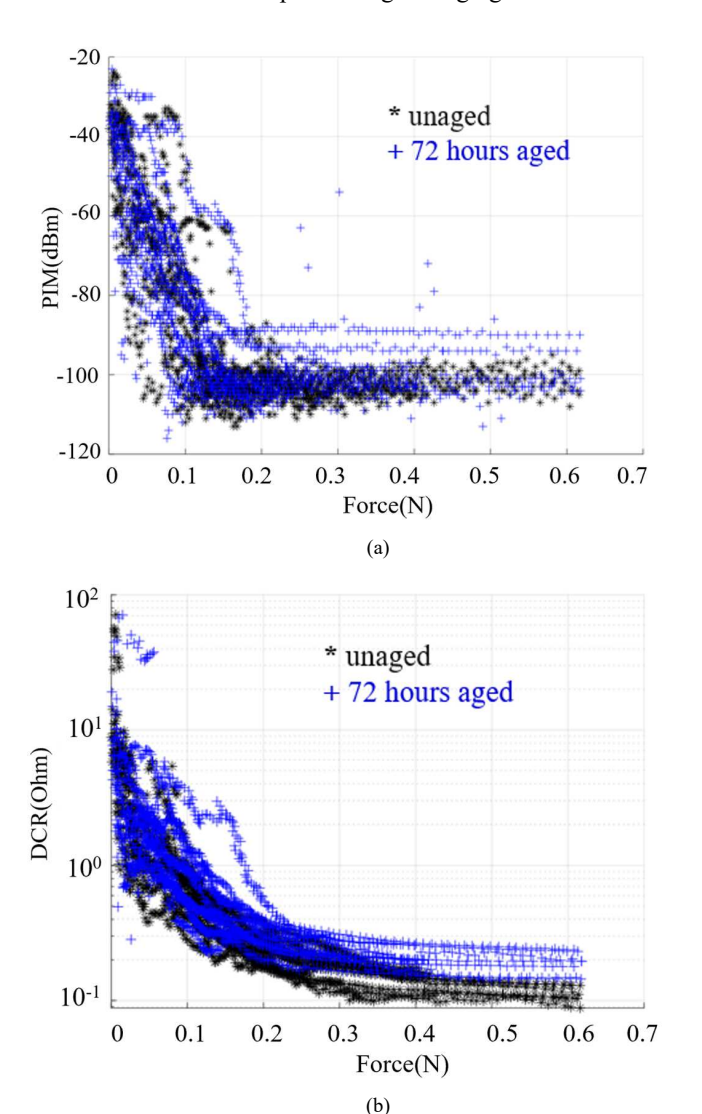


Fig. 7. Fresh and aged data comparison for continuously aged FOF for 72 hours (a) PIM-force (b) DCR-force.

A static I-V based PIM evaluation is adapted from [11] to estimate the PIM level before and after aging the samples to compare with the actual measured PIM level as shown in Fig. 8. The estimation technique was implemented by gradually sweeping the current and obtaining a static I-V curve. The curve is then fitted, and the coefficients were extracted to calculate the corresponding PIM level. The method estimated the actual

PIM level effectively before aging and did not capture the spikes after aging due to the additional current path from the unintentional tail-upper landing pad contact.

With the unintentional tail-landing pad contact, an additional current path was created which potentially affects signals as the desired frequency gets higher. This unintentional current path had an impact only on the RF signals and the DC resistance was not affected. DC measurements do not have the capability to capture multiple current paths and thus a static I-V based PIM evaluation cannot be implemented to estimate the PIM level for such cases.

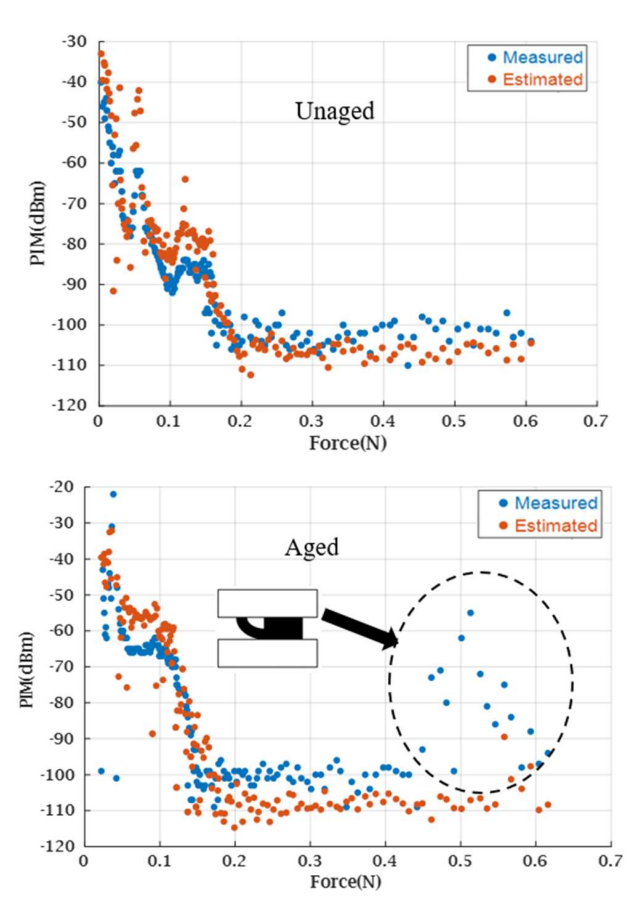


Fig. 8. Static I-V based PIM estimation before and after aging.

To further understand the changes in the contact DC resistance of the FOFs, microscopic images of the conductive fabric surface were taken using scanning electron microscopy (SEM). Fig. 9 shows these microscopic images for unaged and aged samples. There was no significant change on the surface of the material observed after the seventy-two hours of elevated TRH aging process.

In addition to the SEM, an EDS analysis was conducted to see the variation in elemental composition of the surface. The chemical reaction between elements found in the environment specifically oxygen and the polymers used in making FOF surface resulted in an oxide formation. Thus, the composition of nickel oxygen was compared before and after undergoing aging in Fig. 10.

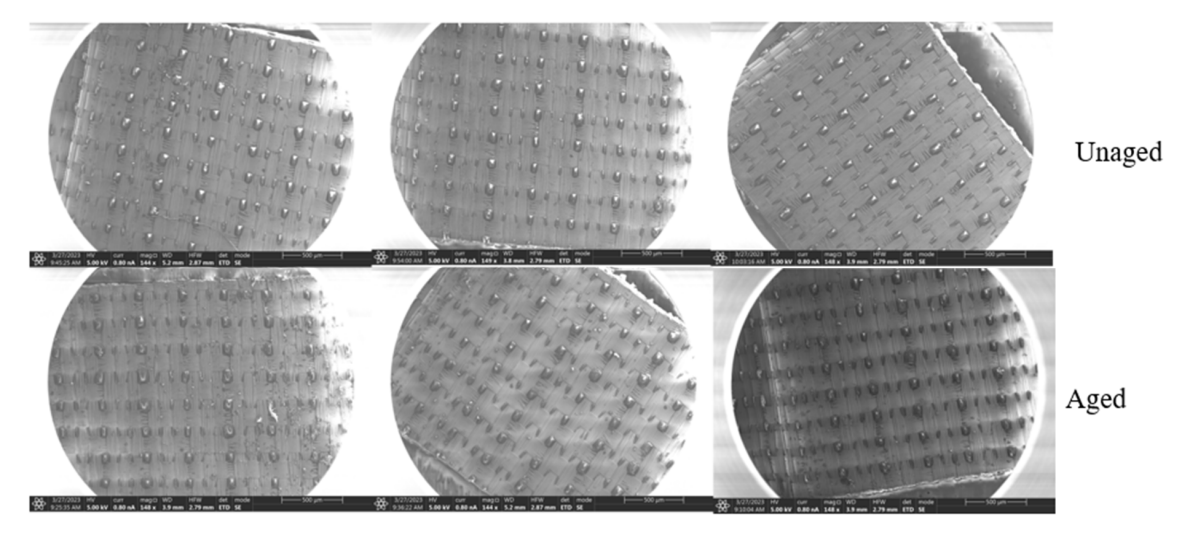


Fig. 9. Microscopic images for the conductive fabric surface of FOF using SEM for unaged and aged samples.

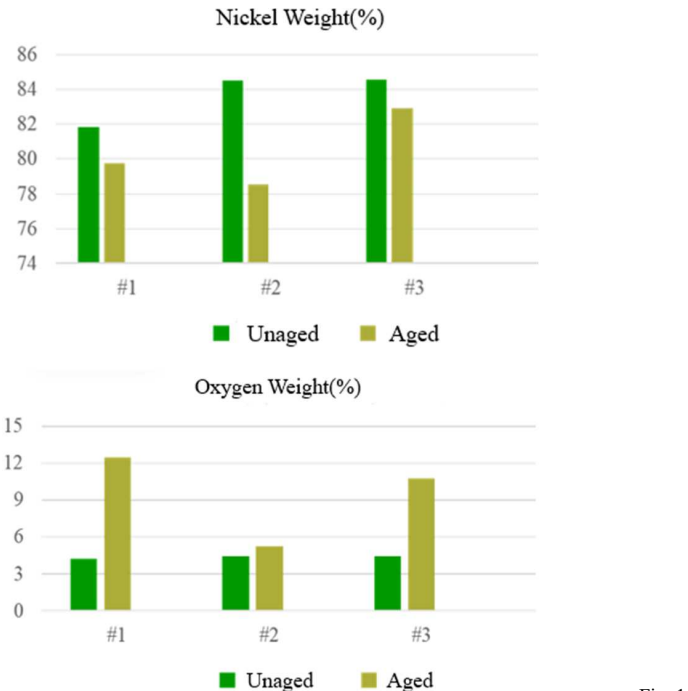


Fig. 10. Elemental composition of the conductive surface of the FOF using EDS analysis

After the FOF went through elevated TRH environmental aging, a growth in oxygen composition was observed indicating an oxide layer formation on the surface of the FOF. However, the actual oxide layer formed on the surface highly depends on the reaction between polymers of the FOF with environmental oxygen [12]. The DC resistance increment observed during measurement was thought to be due to this oxide formation.

The next data shown in Fig. 11 is the force-step curve to understand the change in the hardness of the FOF throughout the aging process. The results show that the FOFs become softer after aging.

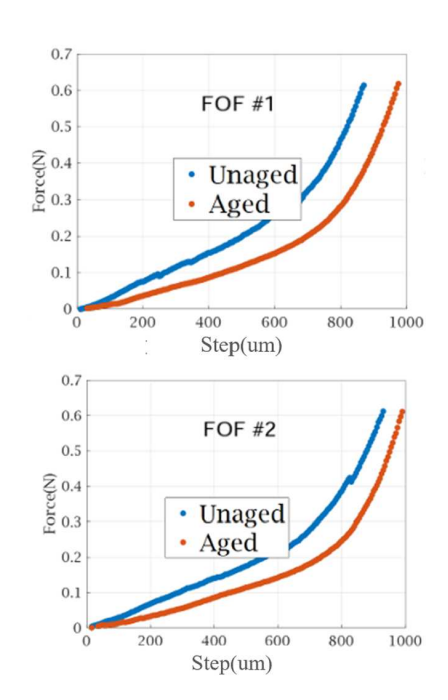


Fig. 11. Force-step curve of FOF before and after aging

IV. CONCLUSION

An elevated TRH environmental aging test was conducted for seventy-two hours to understand the variation in PIM and contact DC resistance to characterize the aging of FOFs. The temperature and RH were set to be 65 °C and 90% respectively. The measured results demonstrate that PIM level variation could be caused by weakened adhesive contact and a DC resistance increase due to an oxide formation on the surface of FOF throughout aging. Experimental results also showed that the FOF material gets softer throughout aging. While this study focused on FOFs coated with nickel, exploring other Fabric over Foams (FOFs) coated with metals possessing different wear and corrosion resistance could yield different outcomes.

There is a significant opportunity for further research into studying the aging characteristics of other metallic contact materials used in today's electronics.

REFERENCES

- [1] S. Yang, W. Wu, S. Xu, Y. Zhang, D. Stutts, and D. Pommerenke, "A passive intermodulation source identification measurement system using a vibration modulation method," *IEEE Trans. Electromagn. Compat.*, vol. 59, no. 6, pp. 1677–1684, May 2017.
- [2] J. R. Wilkerson, I. M. Kilgore, K. G. Gard, and M. B. Steer, "Passive intermodulation distortion in antennas," *IEEE Trans. Antennas Propag.*, vol. 63, no. 2, pp. 474–482, Feb. 2015.
- [3] P. L. Lui and A. D. Rawlins, "Passive non-linearities in antenna systems," in *Proc. IEE Colloq. Passive Intermodulation Products* Antennas Related Struct. Tech. Dig., London, U.K., pp. 6–7, Jun. 1989.
- [4] X. Chen, S. Yang, D. J. Pommerenke, Y. He, M. Yu and J. Fan, "Compact Intermodulation Modulator for Phase Reference in Passive Intermodulation Measurements," *IEEE Transactions on Instrumentation and Measurement*, vol. 68, no. 12, pp. 4612-4614, Dec. 2019
- [5] Nan E. Butler et al., "Effects of surface roughness and aging on the electrical contact resistance and residual stress in gold-nickel-copper connector material", M. S. thesis, The Pennsylvania State University of State College, PA, 2014.

- [6] R.R. Bonaldi, "Electronics used in high-performance apparel 12a" in High-Performance Apparel, Woodhead publishing, Sawaston, UK. 2018
- [7] Nickel plating handbook, 1st ed. The Nickel Institute, Durham, North Carolina, U.S.A., 2013
- [8] P. Faraji, J. L. Drewniak, D. S. McBain and D. Pommerenke, "SE measurements with a TEM cell to study gasket reliability," 2013 IEEE International Symposium on Electromagnetic Compatibility, Denver, CO, USA, 2013, pp. 462-465.
- [9] S. Xia, et al., "Practical Fixture Design for Passive Intermodulation Tests for Flexible Metallic Contacts," 2022 IEEE International Symposium on Electromagnetic Compatibility & Signal/Power Integrity (EMCSI), 2022, pp. 17-22
- [10] S. Xia, et al., "Gassian Process Regression Analysis of Passive Intermodulation Level and DCR for Spring Contacts," 2021 IEEE International Joint EMC/SI/PI and EMC Europe Symposium, 2021, pp. 935-939
- [11] Kalkidan W. Anjajo, et al., "Static I-V based PIM Evaluation for Spring and Fabric-over-Foam Contacts" 2023 IEEE International Symposium on Electromagnetic Compatibility & Signal/Power Integrity (EMCSI), 2023
- [12] Choi SB, et al, "Role of Oxygen in the Ti₃AlC₂ MAX Phase in the Oxide Formation and Conductivity of Ti₃C₂-Based MXene Nanosheets", ACS Appl Mater Interfaces. 2023 Feb 15;15(6):8393-8405